



Article

# A Data Driven approach for the measurement of $^{10}\text{Be}/^9\text{Be}$ in Cosmic Rays with magnetic spectrometers.

Cinzia Cernetti <sup>1</sup> and Francesco Nozzoli <sup>2\*</sup> <sup>1</sup> Trento University, via Sommarive 14 I-38123 Trento, Italy<sup>2</sup> INFN-TIFPA, Via Sommarive 14 I-38123 Trento, Italy

\* Correspondence: Francesco.Nozzoli@unitn.it

**Abstract:** Cosmic Rays (CR) are a powerful tool for the investigation of the structure of the magnetic fields in the galactic halo and the properties of the Inter-Stellar Medium. Two parameters of the CR propagation models: the galactic halo (half-) thickness,  $H$ , and the diffusion coefficient,  $D$ , are loosely constrained by current CR flux measurements, in particular a large degeneracy exist being only  $H/D$  well measured. The  $^{10}\text{Be}/^9\text{Be}$  isotopic flux ratio (thanks to the 2 My lifetime of  $^{10}\text{Be}$ ) can be used as a radioactive clock providing the measurement of CR residence time in the galaxy. This is an important tool to solve the  $H/D$  degeneracy. Past measurements of  $^{10}\text{Be}/^9\text{Be}$  isotopic flux ratio in CR are scarce, limited to low energy and affected by large uncertainties. Here a new technique to measure  $^{10}\text{Be}/^9\text{Be}$  isotopic flux ratio, with a *Data-Driven* approach, in magnetic spectrometers is presented. As an example by applying the method to Beryllium events published by PAMELA experiment it is now possible to determine the important  $^{10}\text{Be}/^9\text{Be}$  measurement avoiding the prohibitive uncertainties coming from the Monte Carlo simulation. It is shown how the accuracy of PAMELA data permits to infer a value of the halo thickness within 25% precision.

**Keywords:** astroparticle physics; cosmic rays; galactic halo

## 1. Introduction

Cosmic Rays (CR) are a powerful tool for the investigation of exotic physics/astrophysics: high energy CR composition provides information on the mysterious galactic PeVatrons and the small anti-matter component in CR could identify the Dark Matter annihilation in our Galaxy.

Besides that, also the structure of the magnetic fields in the galactic halo and the properties of the Inter-Stellar Medium can be probed by detailed CR flux measurements. In particular the ratio of secondary CR (as Li, Be, B) over the primary CR (as He, C, O) is able to provide the *grammage*, that is the amount of material crossed by CR in their journey through the Galaxy.

Two parameters of the CR propagation models: the galactic halo (half-) thickness,  $H$ , and the diffusion coefficient,  $D$ , are loosely constrained by such a *grammage* measurement, in particular a large degeneracy exist being only  $H/D$  well measured [1].

The uncertainties on  $D$  and  $H$  parameters (this last one is known to be in the range 3-8 kpc) also reflects on the accuracy of the determination of secondary anti-proton and positrons fluxes that are the background for the Dark Matter or exotic (astro-)physics searches [2–5].

Abundances of long living unstable isotopes in CR can be used as a radioactive clock providing the measurement of CR residence time in the Galaxy. This time information is complementary to the crossed *grammage*, thus abundance of radioactive isotopes in CR is an important tool to solve the existing  $H/D$  degeneracy in CR propagation models.



Citation: . Proceedings 2021, 1, 0.

<https://doi.org/>

Received:

Accepted:

Published:

**Publisher's Note:** MDPI stays neutral with regard to jurisdictional claims in published maps and institutional affiliations.



**Copyright:** © 2020 by the authors. Licensee MDPI, Basel, Switzerland. This article is an open access article distributed under the terms and conditions of the Creative Commons Attribution (CC BY) license (<https://creativecommons.org/licenses/by/4.0/>).

### 1.1. Beryllium isotopic measurements in Cosmic Rays

Only few elements in cosmic rays: Be, Al, Cl, Mg, Fe contains long-living radioactive isotopes, among them the Beryllium is the lighter, i.e. the most promising for a measurement of isotopic composition in the relativistic kinetic energy range. Three Beryllium isotopes are found in cosmic rays:

- ${}^7\text{Be}$ : stable as bare nucleus in CR. On Earth it decays by electron capture ( $T_{1/2} = 53$  days).
- ${}^9\text{Be}$ : stable.
- ${}^{10}\text{Be}$   $\beta$ -radioactive nucleus ( $T_{1/2} = 1.39 \times 10^6$  years).

The missing  ${}^8\text{Be}$  has a central role in the stellar and Big-Bang nucleosynthesis, the extremely short half-life ( $8.19 \times 10^{-17}$  s) represents a bottleneck for an efficient synthesis of heavier nuclei in the Universe. From the measurement point of view this "isotopic-hole" in the Beryllium mass spectrum is very useful to determine the large amount of  ${}^7\text{Be}$  and to reduce the contamination in the identification of  ${}^9\text{Be}$  and  ${}^{10}\text{Be}$ .

The identification of Beryllium isotopes in magnetic spectrometers requires the simultaneous measurement of particle rigidity,  $R = p/Z$ , and velocity  $\beta = v/c$ . This allows the reconstruction of the particle mass  $m = RZ/(\gamma\beta)$ .

The typical mass resolution of magnetic spectrometers onboard past or current CR experiments ( $\delta M \simeq 0.4 - 1$  amu) does not allow for an event-by-event isotope identification, therefore the "traditional" approach for the measurement of Beryllium isotopic abundances rely on the comparison of the experimental mass distribution with a Monte Carlo simulation.

This approach requires a very well tuned Monte Carlo simulation of the experiment and the possible small residual discrepancies with the real detector response could prevent the measurement of the (interesting-) small amount of  ${}^{10}\text{Be}$ .

This systematics is well described in [6] where the "Monte-Carlo-based" analysis of Beryllium events collected by the PAMELA experiment allows only the measurement of  ${}^7\text{Be}/({}^9\text{Be}+{}^{10}\text{Be})$ .

In the following a *Data-Driven* approach for the measurement of Beryllium isotopic abundances with magnetic spectrometers is described, this can evade the systematics related to Monte Carlo simulation. In particular, as an example, the application of this new approach to PAMELA Beryllium event counts, gathered from fig. 3 and fig 4 of [6] is shown and a preliminary measurement of  ${}^{10}\text{Be}/{}^9\text{Be}$  in the 0.2-0.85 GeV/n range is provided.

## 2. Data-Driven analysis

Knowing the true value of Beryllium isotope masses and a physically motivated scaling of the mass resolution for the three Beryllium isotopes, the shape of the isotope mass distributions can be retrieved, by self-consistency, solely from measured data.

In particular the expected mass resolution for a magnetic spectrometer is:

$$\frac{\delta M}{M} = \sqrt{\left(\frac{\delta R}{R}\right)^2 + \gamma^4 \left(\frac{\delta \beta}{\beta}\right)^2} \quad (1)$$

Typically the isotopic measurement is pursued in kinetic energy/nucleon bins (i.e. in  $\beta$  bins) therefore the velocity contribution to mass resolution is constant for the different isotopes.

Moreover, in the (low-)kinetic energy range accessible by current isotopic measurements, the rigidity resolution is dominated by multiple Coulomb scattering, i.e.  $\delta R/R$  is practically constant for the different isotopes.

Finally, the masses of the three Be isotopes are within 30%, therefore for a fixed  $\beta$  value the rigidity values for different Be isotopes are within 30%; for this reason, with a very good approximation,  $\delta M/M$  is constant and we can assume that  $\text{RMS}(M)/\langle M \rangle$  is the same for the three unknown mass distributions (hereafter also named *templates*).

### 2.1. Template Transformations

We can define  $T_7$ ,  $T_9$  and  $T_{10}$  the unknown normalized templates for  ${}^7\text{Be}$ ,  ${}^9\text{Be}$  and  ${}^{10}\text{Be}$  respectively and  $f_n = {}^n\text{Be}/\text{Be}$  their unknown isotope abundance fractions.

A template  $T_a$  can transform in the template  $T_b$  by applying the operator  $A_{a,b}T_a(x) = T_b(x)$ , and we can assume  $A_{a,b}$  is just transforming the coordinates  $x \rightarrow g(x)$ ; therefore, to ensure template normalization:

$$T_b(x) = A_{a,b}T_a(x) = \frac{dg}{dx}T_a(g(x)) \quad (2)$$

In principle an infinite set of functions  $g(x)$  are able to perform a transformation among two specific templates, however, we are typically interested in monotonic functions preserving quantiles avoiding template folding. A very simple set of transformations are the linear ones  $L_{a,b}$  defined by translation and scale transformations:  $x \rightarrow mx + q$ .

$L_{a,b}$  transforms a normal distribution in a normal distribution.

Defining  $\sigma_a$  the RMS of template  $T_a$  and  $x_a$  the median of template  $T_a$ , the linear transformation  $L_{a,b}T_a = T_b$  is the function:  $x \rightarrow \frac{\sigma_a}{\sigma_b}x + \left[x_a - \frac{\sigma_a}{\sigma_b}x_b\right]$ .

The same transformation applied to a different template  $L_{a,b}T_c = T_d$  provides:  $\sigma_d = \sigma_c \frac{\sigma_b}{\sigma_a}$  and  $x_d = x_b + (x_c - x_a) \frac{\sigma_b}{\sigma_a}$ .

The linear transformation that satisfy the assumption ( $\delta M/M = \text{constant}$ ) is simply:  $x \rightarrow \frac{x_a}{x_b}x$  that is a pure scaling depending only from known Beryllium isotope mass ratios and not from the unknown mass resolution or template shapes.

### 2.2. Data-Driven template evaluation and fit

Defining the known (measured) data distribution  $D(x)$  and assuming as fixed the three  $f_n$ , this system can be considered:

$$\begin{aligned} D(x) &= f_7T_7 + f_9T_9 + f_{10}T_{10} \\ A_{7,9}D(x) &= f_7T_9 + f_9A_{7,9}T_9 + f_{10}A_{7,9}T_{10} \\ A_{7,10}D(x) &= f_7T_{10} + f_9A_{7,10}T_9 + f_{10}A_{7,10}T_{10} \end{aligned} \quad (3)$$

therefore the  ${}^7\text{Be}$  template can be written as:

$$\begin{aligned} T_7 &= \frac{1}{f_7} \left[ D - \frac{f_9}{f_7} A_{7,9}D - \frac{f_{10}}{f_7} A_{7,10}D \right] + \\ &+ \frac{f_9f_9}{f_7^2} T_{G1} + \frac{f_9f_{10}}{f_7^2} T_{G2} + \frac{f_{10}f_9}{f_7^2} T_{G3} + \frac{f_{10}f_{10}}{f_7^2} T_{G4} \end{aligned} \quad (4)$$

where the last four terms, *ghost*-templates, are defined by:

$$\begin{aligned} T_{G1} &= A_{7,9}T_9 \simeq L_{7,x_{G1}}T_7 \\ T_{G2} &= A_{7,9}T_{10} \simeq L_{7,x_{G2}}T_7 \\ T_{G3} &= A_{7,10}T_9 \simeq L_{7,x_{G3}}T_7 \\ T_{G4} &= A_{7,10}T_{10} \simeq L_{7,x_{G4}}T_7 \end{aligned} \quad (5)$$

under the linear approximation the median of *ghost*-templates can be evaluated:

$$\begin{aligned} x_{G1} &= x_9 + (x_9 - x_7) \frac{\sigma_9}{\sigma_7} \simeq 11.5 \text{ amu} \\ x_{G2} &= x_9 + (x_{10} - x_7) \frac{\sigma_9}{\sigma_7} \simeq 13 \text{ amu} \\ x_{G3} &= x_{10} + (x_9 - x_7) \frac{\sigma_{10}}{\sigma_7} \simeq 13 \text{ amu} \\ x_{G4} &= x_{10} + (x_{10} - x_7) \frac{\sigma_{10}}{\sigma_{10}} \simeq 14 \text{ amu} \end{aligned} \quad (6)$$

Profiting that the *ghost*-templates are placed beyond  $T_{10}$  and that we know  $f_7 > f_9 > f_{10}$ , the contribution of *ghost*-templates in equation 4 is small and  $T_7$  can be iteratively evaluated from measured data by using eq. 5 and the linear approximation.

Once  $T_7$  is obtained, also the other templates are straightforwardly obtained by using  $L_{7,9}$  and  $L_{7,10}$  and a  $\chi^2$  value for the fixed  $f_7$ ,  $f_9$  and  $f_{10}$  configuration is obtained by comparison with  $D(x)$ . The best fit value of  $f_7$ ,  $f_9$  and  $f_{10}$  is obtained by minimizing the  $\chi^2$  on the allowed configuration space ( $f_7 + f_9 + f_{10} = 1$ ).

This *Data-Driven* approach have been tested on Monte Carlo simulated events and it is able to correctly retrieve the injected isotopic ratios within statistical fluctuations. In the following the example of application to Beryllium events published by PAMELA experiment [6] is shown.

In figure 1, a  $\chi^2$  map for the  $\langle f_7 \text{ vs } f_{10}/f_9 \rangle$  parameter space is shown for the example of PAMELA-ToF events in the 0.65-0.85 GeV/n range (last bin of our analysis). The best-fit is marked by a red triangle and the 68% confidence interval is surrounded by a red contour.

It is important to note that three naive solutions of the *Data-Driven* analysis are obviously  $f_7 = 1$ ,  $f_9 = 1$  and  $f_{10} = 1$ , these obvious solutions are characterized by  $\chi^2 = 0$ . When statistic is scarce, the bias induced by these naive solutions has a not negligible impact in the physical best-fit position and in the correct confidence interval evaluation. To remove this bias a bootstrap method has been used, i.e. we have simulated 100 pseudo-experiments randomly extracting the data distribution  $D(x)$  from the measured one, following the known Poisson statistics. Therefore the templates coming from *Data-Driven* analysis has been used to extract  $\chi^2$  map from each pseudo-experiment and the fig. 1 is showing the unbiased  $\chi^2$  map obtained by average of  $\chi^2$  maps of the 100 pseudo-experiments. In this way the unbiased  $\chi^2$  obtained by the three naive solution is non-zero and is similar to the one obtained by the unbiased physical solution.

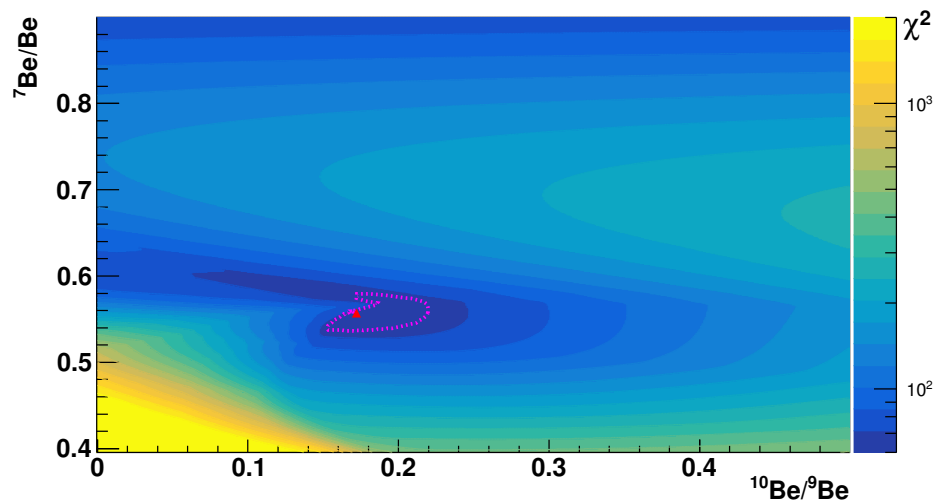


**Figure 1.** Unbiased map of  $\chi^2$  configurations for PAMELA-ToF in the 0.65-0.85 GeV/n region.

In fig. 2 the best-fit for the example of PAMELA-ToF 0.65-0.85 GeV/n region is shown. The templates are obtained with this *Data-Driven* approach.

Finally, it is important to note that the results of this *Data-Driven* approach are identical, by construction, even applying an arbitrary/overall scaling of the reconstructed mass value. For this reason the results obtained by *Data-Driven* analysis are quite solid regarding possible rigidity/velocity scale mis-calibrations that could prevent the *traditional* MC-based analysis as shown in [6]. As a practical example we can apply the *Data-Driven* analysis also to events measured by PAMELA calorimeter (fig. 4 of ref. [6]) even without a tuned Monte Carlo model/calibration for the  $dE/dx$  measurement.

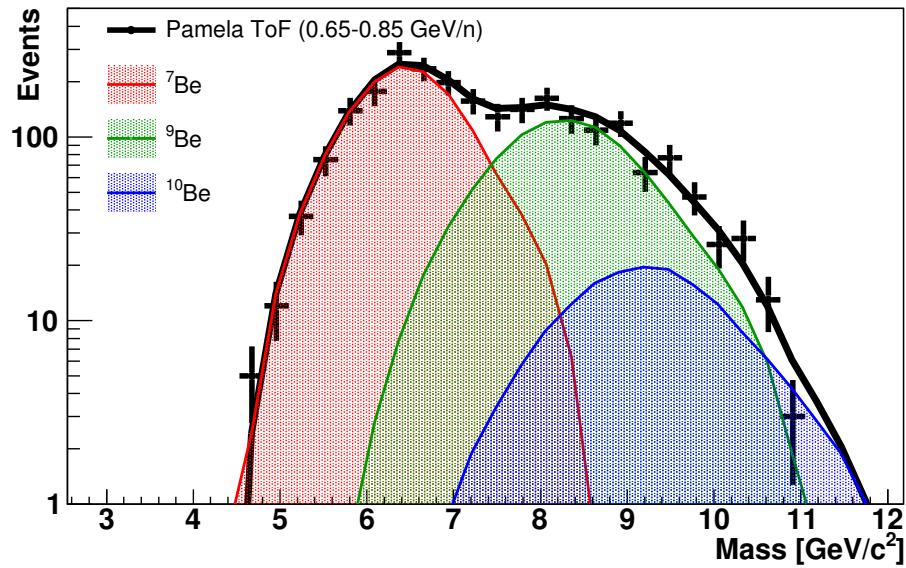


**Figure 2.** Example of Beryllium isotope measurement with the *Data-Driven* analysis of PAMELA-ToF data collected in the 0.65-0.85 GeV/n range.

### 3. Results and discussion

The results of the *Data-Driven* analysis of  ${}^7\text{Be}/\text{Be}$  and  ${}^{10}\text{Be}/{}^9\text{Be}$  fraction using the PAMELA data [6] are shown in figure 3 and compared with previous measurements [7–18].

The measurement obtained by PAMELA-ToF (black dots) is in reasonable agreement with the one obtained with PAMELA-Calorimeter (blue square); for both results only the statistic error bars are shown. A complete evaluation of systematic uncertainties for these results is dominated by the possible differences in the selection acceptance for  ${}^7\text{Be}$ ,  ${}^9\text{Be}$  and  ${}^{10}\text{Be}$ . these cannot be estimated without a Monte Carlo simulation of the detector, however the contribution is expected to be small (few %) in comparison with the wide statistical error bars. In particular, regarding  ${}^7\text{Be}/\text{Be}$ , the results of the *Data-Driven* analysis are in agreement with the ones published in [6] based on the Monte Carlo template fit of the PAMELA data (orange dots) suggesting not dominant systematics.

The new information provided by the *Data-Driven* analysis, when applied to PAMELA data, is a relatively precise estimation of  ${}^{10}\text{Be}/{}^9\text{Be}$  ratio in the range 0.2-0.85 GeV/n where existing measurements are scarce and affected by large uncertainty. In particular it is interesting to note that this measurement is in good agreement with the model of [1,2,4,5] that are recent predictions of  ${}^{10}\text{Be}/{}^9\text{Be}$  tuned with the up-to-date AMS-02 fluxes (and previous low-energy  ${}^{10}\text{Be}/{}^9\text{Be}$  measurements).

The precision of PAMELA data improves the knowledge of  ${}^{10}\text{Be}/{}^9\text{Be}$  at “large” energy, with a sizable impact in the measurement of the Galactic halo (half-) thickness parameter, currently known in the wide range  $H = 5^{+3}_{-2}\text{kpc}$  [4].

To quantify the sensitivity of PAMELA measurement to halo thickness parameter, the model of [1] is plotted in fig. 3 for different values of  $H$  in the range 1-12 kpc. A simple  $\chi^2$  fit for the model [1] in the sub-range 0.45-0.85 GeV/n provides  $H = 6.5 \pm 1.7$  kpc.

In conclusion, the *Data-Driven* analysis of Beryllium isotope measurement with magnetic spectrometers is useful to reduce the systematics related to the Monte Carlo based analysis. A determination of halo thickness parameter with an error of the order of  $\sim 25\%$  can be achieved, entering in the era of the precision measurements expected by the forthcoming AMS-02 and HELIX results.

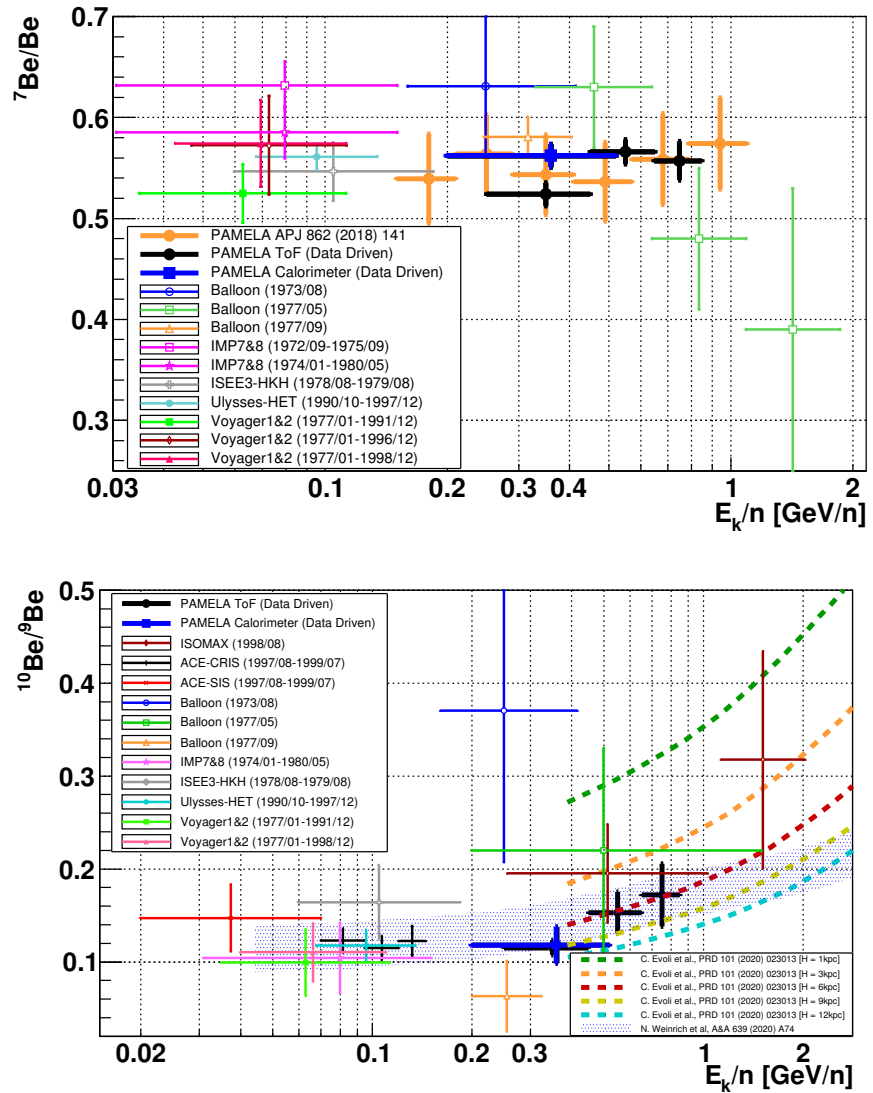


**Figure 3.** Comparison of the results of the *Data-Driven* analysis for  ${}^{10}\text{Be}/{}^9\text{Be}$  and  ${}^7\text{Be}$  fraction with previous experiments and with a Monte Carlo based analysis. Only statistic error bars are drawn for the *Data-Driven* analysis results.

## References

1. C. Evoli et al. AMS-02 beryllium data and its implication for cosmic ray transport. *Phys. Rev. D* **2020**, *101*, 023013.
2. J. Feng, N. Tomassetti and A. Oliva. Bayesian analysis of spatial-dependent cosmic-ray propagation: Astrophysical background of antiprotons and positrons. *Phys. Rev. D* **2016**, *94*, 123007.
3. M. Korsmeier and A. Cuoco. Galactic cosmic-ray propagation in the light of AMS-02: Analysis of protons, helium, and antiprotons. *Phys. Rev. D* **2016**, *94*, 123019.
4. N. Weinrich et al. Galactic halo size in the light of recent AMS-02 data. *A&A* **2020**, *639*, A74.
5. P. de la Torre Luque et al. Implications of current nuclear cross sections on secondary cosmic rays with the upcoming DRAGON2 code. *arXiv:2101.01547*.
6. W. Menn et al. Lithium and Beryllium Isotopes with the PAMELA Experiment. *APJ* **2018**, *862*, 141.
7. N. E. Yanasak et al. Measurement of the Secondary Radionuclides  $^{10}\text{Be}$ ,  $^{26}\text{Al}$ ,  $^{36}\text{Cl}$ ,  $^{54}\text{Mn}$ , and  $^{14}\text{C}$  and Implications for the Galactic Cosmic-Ray Age. *APJ* **2001**, *563*, 768.
8. F. A. Hagen et al. Be-10 abundance and the age of cosmic rays - A balloon measurement. *APJ* **1977**, *212*, 262.
9. A. Buffington et al. A measurement of cosmic-ray beryllium isotopes from 200 to 1500 MeV per nucleon. *APJ* **1979**, *226*, 355.
10. W. R. Webber and J. Kish. Further Studies of the Isotopic Composition of Cosmic Ray Li, Be and B Nuclei-Implications for the Cosmic Ray Age. *Int. Cosm. Ray Conf.* **1979**, *1*, 389.
11. M. Garcia-Munoz, G. M. Mason, and J. A. Simpson. The age of the galactic cosmic rays derived from the abundance of Be-10. *APJ* **1977**, *217*, 859.
12. M. Garcia-Munoz, J.A. Simpson and J.P. Wefel. The propagation life-time of galactic cosmic rays determined from the measurement of the Beryllium isotopes. *Int. Cosm. Ray Conf.* **1981**, *2*, 75.
13. M. E. Wiedenbeck and D. E. Greiner. A cosmic-ray age based on the abundance of Be-10. *APJ Lett.* **1980**, *239*, L139.
14. T. Hams et al. Measurement of the Abundance of Radioactive  $^{10}\text{Be}$  and Other Light Isotopes in Cosmic Radiation up to 2 GeV Nucleon $^{-1}$  with the Balloon-borne Instrument ISOMAX. *APJ* **2004**, *611*, 892.
15. J. J. Connell. Galactic Cosmic-Ray Confinement Time: ULYSSES High Energy Telescope Measurements of the Secondary Radionuclide  $^{10}\text{Be}$ . *APJ Lett.* **1998**, *501*, L59.
16. A. Lukasiak et al. The isotopic composition of cosmic-ray beryllium and its implication for the cosmic ray's age. *APJ* **1994**, *423*, 426.
17. A. Lukasiak, F. B. McDonald, and W. R. Webber. Voyager Measurements of the Isotopic Composition of Li, Be and B Nuclei. *Int. Cosm. Ray Conf.* **1997**, *3*, 389.
18. A. Lukasiak. Voyager Measurements of the Charge and Isotopic Composition of Cosmic Ray Li, Be and B Nuclei and Implications for Their Production in the Galaxy. *Int. Cosm. Ray Conf.* **1999**, *3*, 41.